TWO-DIMENSIONAL ELECTRON DENSITY IMAGING FOR SF_6 ARC INTERRUPTION PHENOMENON USING SHACK-HARTMANN TYPE LASER WAVEFRONT SENSOR

Y. INADA[1]*, T. KAMIYA[1], S. MATSUOKA[1], A. KUMADA[1], H. IKEDA[1] AND K. HIDAKA[1]

[1] Department of Electrical Engineering and Information Systems, The University of Tokyo, 7-3-1 Hongo, Bunkyo-ku, Tokyo, 113-8656, Japan.
*email of corresponding author: inada@hvg.t.u-tokyo.ac.jp

ABSTRACT

Shack-Hartmann type laser wavefront sensors were used for the direct imaging of two-dimensional electron density distributions over SF_6 gas-blast arc discharges with damping sinusoidal arc current waveforms in order to experimentally characterise electron density profiles for the success and failure of arc interruption in the thermal reignition phase. When electron densities at the current zero were locally reduced to less than $10^{21}m^{-3}$ and the axial distributions were seen to be discontinuous, the arc current interruption was successful with a probability of 100%. The undetected electron densities around the tip of the lower electrode were assumed to be $10^{17} \sim {}^{18}m^{-3}$ from the simultaneous arc conductance measurement and numerical studies of electrical conductivity. On the other hand, axially continuous electron densities of more than $10^{21}m^{-3}$ bridging the interelectrode gap drastically degraded thermal interruption performance and caused a failure probability of 86%.

1. INTRODUCTION

When grounding faults occur in power systems, high-voltage SF_6 gas circuit breakers are responsible for extinguishing SF_6 arc plasmas rapidly, removing the line faults and protecting other transmission devices with high reproducibility [1]. In order to develop highly reliable SF_6 gas circuit breakers, it is required to achieve the characterisation of the transient behaviours of SF_6 arc discharges around current zero. However, the SF_6 arc plasmas in current-zero phases are unstable and even under the same experimental conditions, constant thermal interruption performance is not achieved. Therefore, it has been extremely difficult to experimentally understand interruption phenomena of the SF_6 arc discharges around current zero, particularly by using the conventional sensing systems for measuring localised physical quantities.

Recently, Shack-Hartmann type laser wavefront sensors have been developed as novel means of visualizing two-dimensional electron density distributions over poorly reproducible decaying arc channels from single recordings [2-4]. The two-dimensional sensing method is particularly suited for characterising the arc behaviours for the success and failure of arc interruption in the thermal reignition phase.
If the reasons for the differences between the success and failure are found in two-dimensional electron density distributions, such fundamental data on the arc parameters are particularly useful for the optimisation of the electrical, mechanical and hydrodynamic parameters in gas circuit breakers and for the development of complete simulation models [5]. Moreover, electron density measurements are the most important among arc parameter diagnostics because the interruption capability of gas circuit breakers largely depends on electron density distributions over SF_6 arc plasmas around current zero [6, 7].

In this paper, we describe two-dimensional electron density imaging over free-burning SF_6 arc discharges with the same voltage and current waveforms in order to experimentally characterise electron density distributions for the success and failure of arc interruption. Our experimental results showed that the current interruption performance was highly dependent

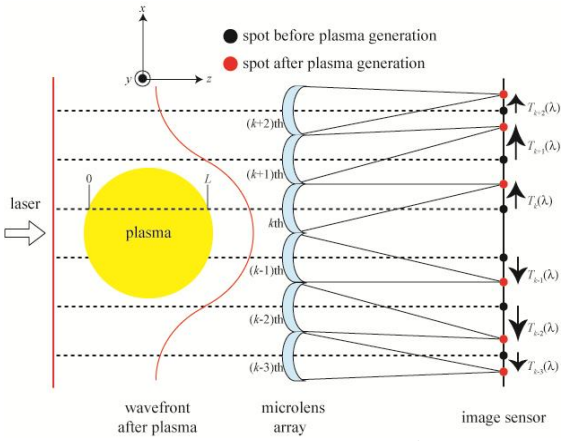

Fig. 1 Shack-Hartmann type laser wavefront sensor.

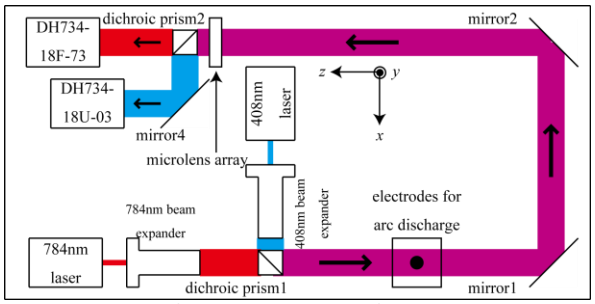

Fig. 2 Top view of the main component of Shack-Hartmann type sensing system.

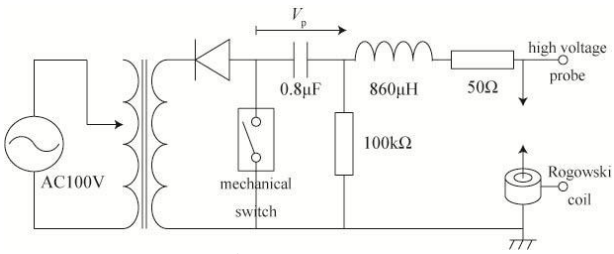

Fig. 3 Circuit for generating arc discharge.

upon the geometric parameters of the SF_6 arc plasmas rather than the absolute values of the electron densities at current zero.

2. EXPERIMENT

A detailed description of electron density measurement using Shack-Hartmann sensors was previously reported [3]. Fig.1 shows the basic concept of a Shack-Hartmann type laser wavefront sensor for measuring an electron density distribution in a plasma. A Shack-Harmann sensor is composed of an image sensor and microlens array converting the localised wavefront gradients of a laser beam into the shifts of the focal spot positions [8-11]. These spot shifts are observed using the image sensor at any given time after plasma generation. The moving distances of the focal spots $T(\lambda)$ for a certain laser wavelength λ have contribution from number densities of neutral particles, positive ions and electrons in the plasma. In particular, only the contribution from electrons depends on λ while that from neutral particles and positive ions is independent of λ. Therefore, our electron density sensing system needs simultaneous measurements of $T(\lambda_1)$ and $T(\lambda_2)$ for two lasers with different wavelengths λ_1 and λ_2. The calculation of $T(\lambda_1)$- $T(\lambda_2)$ is made to eliminate the contribution from neutrals and ions and to extract electron density contribution. The experimental and analytical procedures involved (i) simultaneous spot shift measurements using two lasers with different wavelengths, (ii) calculations of line-integrated electron density profiles using the radial components of the spot shifts, (iii) approximations of the profiles by Gauss functions, and (iv) Abel transformation to the Gauss functions for obtaining the electron density profiles under the assumption of axial symmetry of the arc discharge.

Fig.2 shows the sensing system in this study employing two continuous-wave diode lasers (λ_1=784nm; λ_2=408nm), one sheet of meniscus microlens array (pitch P=300μm; focal length f_1=213mm at λ_1 and f_2=211mm at λ_2) and two ICCD (intensified charge-coupled device) cameras [2]. The spatial resolution of this electron density measuring system was P=300μm in the radial direction x and in the axial direction y of arc plasmas. The temporal resolution was equal to exposure time T_G of the ICCD cameras and it was set to T_G=2μs.

Our Shack-Hartmann sensors have trade-off between measurement sensitivity and temporal resolution. The previously reported measurement sensitivity in the case of $f \sim$ 200mm and T_G=200ns was $10^{22}m^{-3}$ [2]. The combination of $f \sim$ 200mm and T_G=2μs in this study offered measurement sensitivity of $10^{21}m^{-3}$.

The electrical circuit for generating arc discharges is illustrated in Fig.3. A 0.8μF capacitor was charged up to V_p=26kV and through a inductance of 860μH and current limiting resistance of 50Ω, atmospheric SF_6 arc discharges were generated in a 3-mm gap between rod-to-rod tungsten electrodes of 1mm in diameter. The arc currents had a gradually damped oscillatory waveform and the initial peak value was 400A. Success or failure of arc current

interruption was judged around the first current-zero points. In the experimental condition, interruption success or failure occurred randomly at a probability of around 50%. The arc currents and arc voltages were measured by a Rogowski coil and a high voltage probe, respectively. The high voltage probe was connected in parallel to the electrode gap.

The arcs were blasted in the arc axial direction y by the forced convection of SF_6 gas with a pressure of 0.15MPa. The blasting pressure corresponded to SF_6 gas velocities of 100m/s around the gap center in arc-free conditions and the velocity fields were almost axially symmetric.

3. RESULTES AND DISCUSSION

Two types of electron density images were observed at the current-zero points under the same experimental condition. One type of the images shows that the electron densities around the tip of the lower electrode were locally reduced below our sensors sensitivity of $10^{21}m^{-3}$ and the electron density distributions in the axial direction y are seen to be spatially discontinuous, as shown in Fig.4(a). Fig.4(b) shows that the simultaneously measured current and voltage waveforms had damping rates of di/dt=0.27A/μs and dv/dt=0.42kV/μs around the current-zero point, respectively. In the case of the spatially discontinuous electron density images, arc current interruption was successful with a probability of 100%.

The other type shows that the electron densities were higher than $10^{21}m^{-3}$ over the interelectrode gap and the electron density distributions in the axial direction y are seen to be spatially continuous, as shown in Fig.5(a). Fig.5(b) shows that the corresponding current and voltage waveforms had damping rates of di/dt=0.27A/μs and dv/dt=0.47kV/μs around the current zero, respectively. The spatially continuous electron density distributions degraded the thermal interruption performance significantly and caused a failure probability of 86%.

The peak arc voltage just before the current zero in Fig.4(b) was higher than that in Fig.5(b) by V_d=20V. Higher arc voltage for the spatially discontinuous electron density images were assumed to be caused by the locally reduced electron densities around the tip of the lower electrode because the main difference between Fig.4(a) and Fig.5(a) was the electron density values around the tip. V_d=20V was applied to the region around $-1.5 \leqq y \leqq 1.0$mm in Fig.4(a), and the local arc conductance and electric field just before the current zero was calculated to be 0.3A/20V =0.015S and 20V/0.5mm=400V/cm, respectively. Supposing that uniform electrical conductivity was distributed in the cylindrical domain placed in $-1.5 \leqq y \leqq 1.0$mm with a width of 1.0mm and height of 0.5mm, the electrical conductivity was estimated to be 10S/m from the local arc conductance of 0.015S and electric field of 400V/cm. Under the thermal equilibrium condition, the electrical conductivity of 10S/m corresponded to electron densities of $10^{17\sim18}m^{-3}$ [12, 13]. The electron densities of 3 or 4 orders of magnitude lower than those in $-1.5 \leqq y \leqq 1.0$mm of Fig.5(a) were advantageous for achieving great thermal interruption performance.

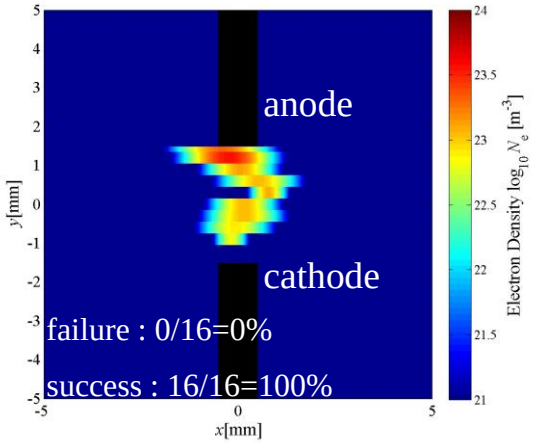

(a) Two-dimensional electron density distribution

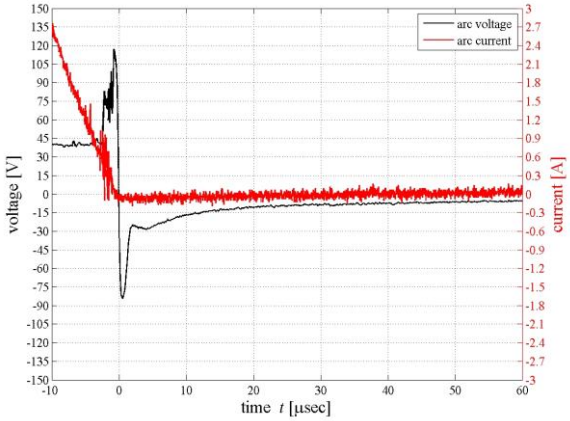

(b) Voltage and current waveform
Fig. 4 Interruption success.

4. CONCLUSION

Shack-Hartmann type laser wavefront sensors

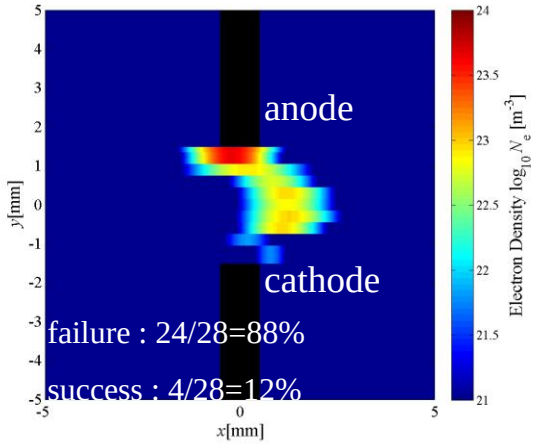

(a) Two-dimensional electron density distribution

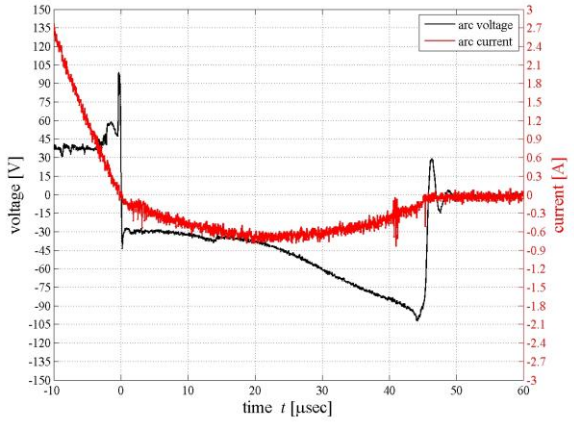

(b) Voltage and current waveform
Fig. 5 Interruption failure.

were used for the direct imaging of two-dimensional electron density distributions over SF_6 gas-blast arc discharges in order to experimentally characterise electron density profiles for the success and failure of arc interruption in the thermal reignition phase. When electron densities at the current zero were locally reduced to less than $10^{21}m^{-3}$, the arc current interruption was successful with a probability of 100%. On the other hand, electron densities of more than $10^{21}m^{-3}$ bridging the gap caused a failure probability of 86%.

REFERENCES

[1] K. Nakanishi, Eds., *Switching Phenomena in High-Voltage Circuit Breakers*, Marcel Dekker, Inc., 1, 1991.

[2] Y. Inada, S. Matsuoka, A. Kumada, H. Ikeda, K. Hidaka, "MEASUREMENT OF 2-DIMENSIONAL ELECTRON DENSITY DISTRIBUTION OVER EXTINGUISHING ATMOSPHERIC ARC USING HIGHLY SENSITIVE SHACK-HARTMANN TYPE LASER WAVEFRONT SENSOR", XIX International Conference on Gas Discharges and Their Applications, A-15, 2012.

[3] Y. Inada, S. Matsuoka, A. Kumada, H. Ikeda, K. Hidaka, "Shack–Hartmann type laser wavefront sensor for measuring two-dimensional electron density distribution over extinguishing arc discharge", J. Phys. D: Appl. Phys., **45**, 435202, 2012.

[4] Y. Inada, S. Matsuoka, A. Kumada, H. Ikeda, K. Hidaka, "Multi-Time Electron Density Imaging over SF_6 and Air Arc Discharge around Current Zero", 31st International Conference on Phenomena in Ionized Gases, PS3-080, 2013.

[5] J. J. Gonzalez, R. Girard and A. Gleizes, "Decay and post-arc phases of a SF_6 arc plasma: a thermal and chemical non-equilibrium model", J. Phys. D: Appl. Phys., **33**, 2759, 2000.

[6] M. T. C. Fang and W. Y. Lin "Current zero behaviour of a gas-blast arc. Part 1: Nitrogen", IEE Proc. A, 1**37**, 175, 1990.

[7] Y. Yokomizu, T. Sakuta and Y. Kito, "A novel approach to AC air arc interruption phenomena viewed from the electron density at current zero", J. Phys. D: Appl. Phys., **22**, 129, 1989.

[8] B. Platt and R. V. Schack "Lenticular hartmann screen", Opt. Sci. Cent. newsl, 5, 15, 1971.

[9] D. Malacara, Eds., *Optical Shop Testing*, Wiley-Interscience, 367, 1978.

[10] T. Fukuchi, Y. Yamaguchi, T. Nayuki, K. Nemoto and K. Uchino, "Development of a Laser Wavefront Sensor for Measurement of Discharge in Air", Electr. Eng. Jpn., 146, 10, 2004.

[11] N. Qi, R. R. Prasad, K. Campbell, P. Coleman, M. Krishnan, B. V. Weber, S. J. Stephanakis and D. Mosher, "Laser wavefront analyzer for imploding plasma density and current profile measurements", Rev. Sci. Instrum., 75, 3442, 2004.

[12] J. J. Gonzalez, A. Gleizes and P. Krenek, "SF_6 circuit breaker arc modeling : influence of the electric field on the electrical conductivity", J. Phys. D: Appl. Phys., **27**, 985, 2004.

[13] W. Z. Wang, M. Z. Rong, Y. Wu, J. W. Spencer, J. D. Yan and D. H. Mei, "Thermodynamic and transport properties of two-temperature SF6 plasmas", Phys. Plasmas, **19**, 083506, 2012.